Appl Biochem Biotechnol (2012) 167:1699–1715
DOI 10.1007/s12010-011-9521-7

Watermelon Rind: Agro-waste or Superior Biosorbent?

Cong Liu · Huu Hao Ngo · Wenshan Guo

Received: 26 October 2011 / Accepted: 21 December 2011 /
Published online: 6 January 2012

Abstract Biosorption of copper (Cu), zinc (Zn), and lead (Pb) on watermelon rind in a well-stirred batch system was investigated. pH showed significant influence on the biosorption process. Optimal pH for Cu, Zn, and Pb biosorption was found to be 5.0, 6.8 and 6.8, respectively. Watermelon rind was in favor of Pb and it could remove up to 99% Pb between pH ranges of 5 and 6.8 when Pb concentration is lower than 100 mg/L. The biosorptive capacity of watermelon on Cu, Zn, and Pb was 6.281, 6.845, and 98.063 mg/g, respectively. The equilibrium data fitted well to Langmuir adsorption isotherm while pseudo-second-order kinetic model exhibited more advantages for describing kinetic data than pseudo-first-order kinetic model. NaOH was found to be a suitable eluent. After desorption in NaOH solution, the resorption efficiency reached as high as 99% of these three metals either in a single-component or multi-component system. From the characterization study, ion exchange and micro-precipitation were estimated to be the main mechanisms. Due to its high metal uptake capacity, reusability, and metal recovery, watermelon rind can be considered as an eco-friendly and economic biosorbent for removing Pb from water and wastewater.

Keywords Watermelon rind · Biosorption · Biosorbent · Heavy metal removal · Model · Desorption

Introduction

Due to the awareness of the hazard of heavy metals, various metals, such as lead, copper, and zinc, have been considered as concerning being dangerous ingredients for humankind and various ecological systems [1–3]. A multitude of processes and methods have been developed for the treatment and disposal of metal-bearing wastewater so as to curtail heavy metal pollution issues (e.g., chemical precipitation, ion exchange, membrane separation, adsorption process, and solvent extraction) [4]. However, all these methods have their respective disadvantages, such as being relatively expensive, generating large amounts of sludge, and involving either elaborate and costly equipment or high cost operation and energy requirements [5]. Therefore,

C. Liu · H. H. Ngo (✉) · W. Guo
Centre for Technology in Water and Wastewater, School of Civil and Environmental Engineering,
University of Technology Sydney, Broadway, Sydney, NSW 2007, Australia
e-mail: h.ngo@uts.edu.au

there is an urgent need for the development of more cost-effective and environmentally friendly methods [6].

Extensive researches have been carried out in an ongoing effort to develop a better treatment for water and wastewater containing toxic heavy metals [6–9]. A number of innovative methods have been used to remove heavy metals, such as biosorption [6], biosorption onto purified biopolymers [7], adsorptive filtration using coated sands [8], and biosorption on magnetic iron oxides [9]. Among these methods, biosorption has aroused most interests as it is a process which employs inexpensive dead biomass to sequester heavy metals from aqueous solutions, especially useful for the removal of trace amounts of heavy metals [6]. The major advantages of biosorption include low cost, high efficiency of heavy metal removal from diluted solutions, cost-effective and simple regeneration of the biosorbent, the possibility of metal recovery, and having no nutrient requirements [4, 5].

Due to its excellent prospect, numerous materials have been studied for the development of cheaper and more effective biosorbents [4, 10]. Generally, the first step for developing a suitable biosorbent is the selection of optimal pretreatment conditions and determination of optimal physicochemical conditions, especially pH of solution [11]. As another fundamental step, the investigation of kinetic models and adsorption isotherms can give important information regarding the uptake mechanism and the possibility of industrial-scale application [11]. Besides, it is also necessary to study the desorption process so as to determine the reusability of these novel biosorbents and the recovery of heavy metals.

Watermelon rind, a common agricultural by-product, is a natural and rich source of the non-essential amino acid citrulline, containing abundant carboxyl and amino groups, which has remarkable capability of binding heavy metals from aqueous solutions [12]. Meanwhile, the study of US Department of Agriculture, Agricultural Research Service [13] indicates that only half of a watermelon fruit is edible while the other half, consisting of about 35% rind and 15% peel, goes to waste. Thus, to reduce agro-waste from watermelon and to discover a new biosorbent, a study on the possible use of watermelon rind as a novel biosorbent for heavy metal removal was necessary.

This work aims to investigate the biosorption and desorption of Cu, Zn, and Pb in water using watermelon rind as a novel biosorbent. Adsorption isotherms and kinetic models were studied to describe the experimental data. Three rounds of biosorption–desorption cycle were conducted to study metal recovery and biosorbent reusability. These results would contribute to a better understanding of biosorption performance of watermelon rind.

Experimental

Materials

Watermelon rind was collected from a local market. The collected watermelon rind was washed with tap water and then rinsed with distilled water. Subsequently, watermelon rind was cut into small pieces, dried, and grounded into powder before its use in biosorption experiments. The drying experiments were carried out in a laboratory scale oven. Dried watermelon rind was stocked in a desiccator at room temperature (20 ±1 °C).

Experimental Condition

All the chemicals used in this study were of analytical grade. Stock solutions of metal ions were prepared in MilliQ water. During the biosorption experiments, stock solutions were

diluted to the specified concentration. Watermelon rind was contacted with each solution at pH 6.48 ±0.1 (the pH of tap water). The reaction mixture was agitated at 125 rpm on a shaker. Agitation contact time was kept for 10 h, which was sufficient to reach equilibrium. All the samples from the experiments were filtered through a 0.45-μm nylon membrane filter and the filtrate was kept for analysis. Biosorption experiments were conducted in triplicate and average values were used for discussion. The whole experiment was conducted at room temperature (20 ±1 °C).

Effect of pH

The effect of initial solution pH, ranging from 2 to 7, was determined by agitation of 0.5 g of watermelon rind and 1 L of metal standard solution at a concentration of 10 mg/L. Before the experiment, the pH was adjusted by adding 0.1 mol/L NaOH or HNO_3 and pH was measured using a pH meter. The experiment conditions were kept the same during the biosorption process.

Effect of Co-ions

In order to study the effect of co-ions during the biosorption process, competitive biosorption of Cu, Zn, and Pb from solutions containing these three metals was investigated. The solution (1 L) containing 10 mg/L of each metal was contacted with 0.5 g of biosorbents and the same experiment conditions were used during the biosorption process.

Isotherm Experiments

The equilibrium isotherms were determined by contacting a constant mass 0.5 g of watermelon rind with 1 L standard solution at a range of different concentrations from 5 to 300 mg/L. A pH value of 6.48 was maintained throughout the experiment by adding 0.1 mol/L NaOH or HNO_3. Langmuir and Freundlich adsorption isotherms were used for estimation and comparison. The experiment conditions were kept the same during the biosorption process.

Kinetic Studies

A kinetic study with different time intervals (5, 10, 15, 20, 25, 30, 45, and 60 min) having fixed metal concentration (10 mg/L), biosorbent amount (0.1 g), and biosorbent particle size (<150 μm) was performed. Also, kinetic infinity biosorption was carried out for 10 h. Pseudo-first-order kinetic model and pseudo-second-order kinetic model were investigated to describe the results. The experiment conditions were kept the same during the biosorption process.

Desorption Studies

To investigate the possibility of repeated use of the biosorbents, desorption experiments were conducted. After biosorption experiments, the metal-loaded biosorbent was transferred and agitated with 1 L of various eluant solutions (e.g., distilled water, 0.1 mol/L NaOH, 0.5 mol/L HNO_3, and 0.5 mol/L HCl) for 10 h. It was again filtered, and then the concentrations of metal ions desorbed in the filtrate were determined. The eluted biosorbent was washed several times with distilled water to remove excess alkali and acid. The biosorbent

regenerated was then used in the next biosorption process. Three rounds of biosorption–desorption cycle were conducted and the experiments were operated under the same conditions during the whole process.

Analysis

Zn, Pb, and Cu concentrations were measured using contrAA 300 atomic adsorption spectrophotometer. Before measurement, the solutions containing metals were appropriately diluted with deionised water to ensure that the concentrations in the sample were linearly dependent on the absorbance detected so as to avoid unexpected errors.

Study of Adsorption Isotherms

In this study, both Langmuir [14] and Freundlich [15] adsorption isotherms were used to describe equilibrium data. The Langmuir equation has the form:

$$q_m = \frac{q_e K_a C_e}{1 + K_a C_e} \tag{1}$$

where q_e=the amount of metal adsorbed at equilibrium (mg/g), q_m=the amount of metal per unit weight of adsorbent to form a complete monolayer on the surface (mg/g), C_e=the equilibrium concentration (mg/L), and K_a=a constant related to the energy of biosorption (L/mg).

Getting the reciprocal of Eq. 1 and moving C_e to the left side of the equation, the parameters (K_a, q_m) of the Langmuir equation can be determined from a linearized form of Eq. 1:

$$\frac{C_e}{q_e} = \frac{1}{q_e K_a} + \frac{C_e}{q_m} \tag{2}$$

The Freundlich model has the form:

$$q_e = K_F \times C_e^{1/n} \tag{3}$$

where K_F=Freundlich isotherm capacity constant and $1/n$=Freundlich isotherm intensity constant.

Then, take the logarithm of both sides of Eq. 3; K_F and n can be determined from a linearized equation as:

$$\log(q_e) = \frac{\log(c_e)}{n} + \log(K_F) \tag{4}$$

Besides the above two normal biosorption isotherms, there is one more isotherm that is commonly used as Redlich–Peterson isotherm [16], which contains three constants and involves the features of both the Langmuir and the Freundlich isotherms. It can be described as:

$$q_e = \frac{A \times C_e}{1 + BC_e^g} \tag{5}$$

where A=Redlich–Peterson isotherm constant, B=Redlich–Peterson isotherm constant, and g=Redlich–Peterson isotherm constant ($0<g<1$).

Then, take the natural logarithm of both sides of Eq. 5 and the latter can be transformed to:

$$\mathrm{Ln}\left(A \times \frac{C_e}{q_e} - 1\right) = g \times \mathrm{Ln}(C_e) + \mathrm{Ln}(B) \tag{6}$$

Although a linear analysis is not possible for a three-constant isotherm, three isotherm constants, A, B, and g, can be evaluated from the pseudo-linear plot using a trial-and-error optimization method. MATLAB program can be developed to determine the correlation coefficient r^2 for a series of values of A for linear regression of Ln (C_e) on Ln [$A \times (C_e/q_e) - 1$], which, subsequently, yields the best value of A and a maximum optimized value of r^2. After that, g and B can also be determined from the linear regression.

Study of Kinetic Models

Two relatively simple rate models known as pseudo-first-order [16, 17] and pseudo-second-order [18–20] kinetic models were investigated to describe the experimental data. The first model is also known as the Lagergren equation and takes the form:

$$\frac{dq_t}{dt} = K_1 \times (q_e - q_t) \tag{7}$$

where q_e=the amount of adsorbed metal ions on biosorbent at the equilibrium (mg/g), q_t= the amount of adsorbed metal ions on biosorbent at any time t (mg/g), and K_1=Lagergren rate constant of the first-order biosorption (g/mg min).

After integration and applying boundary conditions t=0 to t=t and q_t=0 to q_t=q_t, the integrated form of the equation becomes:

$$\log(q_e - q_t) = \log\ q_e - K_1 t \tag{8}$$

When the values of log ($q_e - q_t$) were linearly correlated with t, the plot of log ($q_e - q_t$) versus t will give a linear relationship from which K_1 and q_e can be determined from the slope and intercept of the graph, respectively.

The second-order kinetic model considered here is given as:

$$\frac{dq_t}{dt} = K_2 \times (q_e - q_t)^2 \tag{9}$$

where K_2=the rate constant of second-order biosorption (g/mg min).

For the boundary conditions, t=0 to t=t and q_t=0 to q_t=q_t, the integrated form of Eq. 9 becomes:

$$\frac{1}{q_e - q_t} = \frac{1}{q_e} + K_2 t \tag{10}$$

which is the integrated rate law for a pseudo-second-order reaction. Equation 9 also has a linear form as:

$$\frac{1}{qt} = \frac{1}{K_2 q_e^2} + \frac{t}{q_e} \tag{11}$$

where h (mg/g/min) can be regarded as the initial sorption rate as $qt/t \rightarrow 0$; hence,

$$h = K_2 q_e^2 \tag{12}$$

Furthermore, Eq. 12 can be written as:

$$\frac{t}{q_t} = \frac{1}{h} + \frac{t}{q_e} \tag{13}$$

If the pseudo-second-order kinetics is applicable to the experimental data, the plot of t/q_t versus t of Eq. 13 should give a linear relationship from which q_e, K_2, and h can be determined from the slope and intercept of the plot, respectively.

Chi-Square Nonlinear Regression

Chi-square calculations are used to compare observed and expected values [21]. Usually, these calculations are used in the context of categorical outcomes, to compare observed and expected distribution of subjects among the categories. The use of chi-square in nonlinear regression is quite different. Regression finds the curve that minimizes the scatter of points around the curve. Based on the scatter of the data, the amount of scatter can be compared with the amount that can be observed and reduce the result to a chi-square value. If this chi-square value is high, then the scatter around the curve is larger, which means that the data do not fit the model well. Nonlinear regression minimizes the sum of the squared vertical distances between the data point and the curve.

To find the best-fit values of the parameters, nonlinear regression minimizes the sum-of-squares. The value of sum-of-squares can be used to compute χ^2. This value is computed by comparing the sum-of-squares with the total variation in Y values. The approach to normalizing the sum-of-squares value is to compare the observed scatter of the points around the curve with the amount of experimental scatter you expect to see based on theory. This can be done by computing chi-square using this equation:

$$\sum\nolimits_1^n \chi 2 = \sum\nolimits_1^n (Y_{\text{data}} - Y_{\text{curve}})^2 / Y_{\text{curve}} \tag{14}$$

Then, non-linear regression coefficient χ^2 can be obtained.

SEM Characterization of Biosorbent

The biosorbent was characterized with the intent of assessing its various physical properties, such as surface structure, so that a better explanation of biosorption mechanism could be provided. In this study, the surface morphology was visualized by using a scanning electron microscope (SEM). The SEM micrographs for the sample were obtained at×1,000 or×2,000 magnification.

BET Characterization of Biosorbent

The surface areas of various biosorbents (e.g., raw biosorbent, biosorbent after biosorption process, and biosorbent after NaOH desorption process) were determined by BET method at a temperature of 77.30 K of liquid nitrogen. The measurement was carried out with Autosorp-1-C instrument, Quantachrome, and the measurement method was nitrogen adsorption and desorption method. The BET surface area, micro-pore area, micro-pore volume, and mean micro-pore diameter were determined at relative pressure (P/P_0) equaled to 1.

Results and Discussion

Effect of pH

Among various influencing factors, the solution pH usually plays a critical role in biosorption, which can affect the solution chemistry of metals and the activity of the functional groups of the biosorbents and can even completely alternate the activity of binding sites [22]. Besides, for metals ions, the speciation and biosorption availability can also be strongly affected by solution pH [22]. Under the condition of higher solution pH, the solubility of metal complexes decreases sufficiently, which, subsequently, leads to precipitation, complicating the biosorption process to a great extent [22]. In this study, the effect of pH was studied in the range from 2 to 6.8. As shown in Fig. 1, the maximum uptake of Cu took place at pH 5. The uptake of Cu increased with increasing solution pH from 2.0 to 5.0 and then showed a slightly decreasing trend when pH was higher than optimal pH. As can be seen from the effect of pH, ion exchange can be dominant in the biosorption of metal ions on watermelon rind; therefore, at lower pH values, the biosorption capacities were low because of the competition between the large quantities of proton and metal ions for surface active sites. As the pH increased, the competition became less fierce and removal efficiency then increased [23]. However, when pH increased over 7, the formation of metal hydroxide complexes should decrease the concentration of free metal ions; thereby, the biosorption capacity became difficult to estimate [24]. For the biosorption of Zn and Pb, similar trends were found and the maximum uptake of Zn and Pb both occurred at pH 6.8. Besides, it was also found that the uptake of Cu and Zn could be more easily affected by pH alteration than

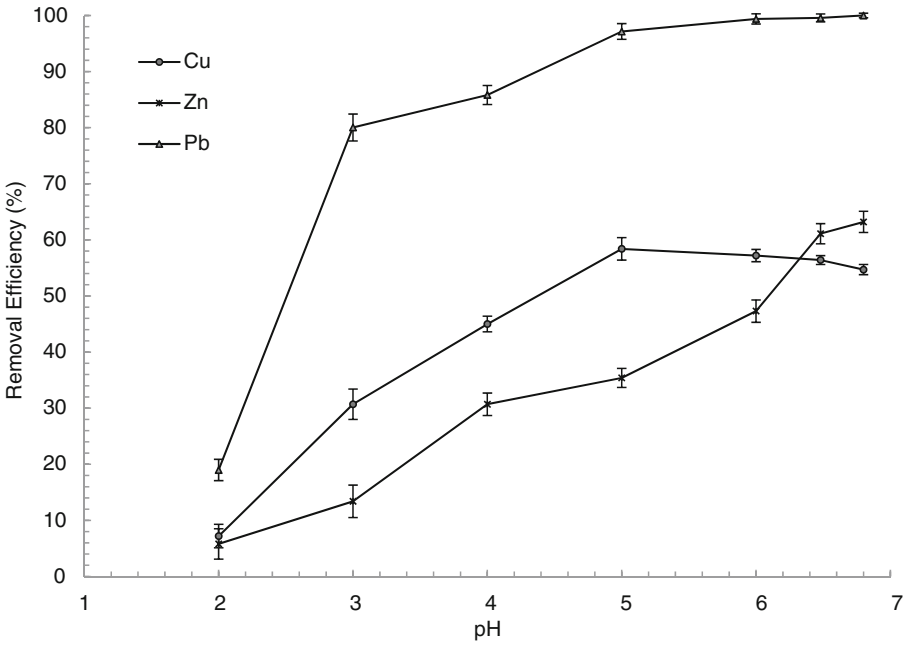

Fig. 1 Effect of solution pH on removal efficiency using watermelon rind as a novel biosorbent in single-metal solution (dosage, 0.5 g; initial metal concentration, 10 mg/L; particle size, <150 μm; contact time 10 h; 125 rpm; 20 °C)

the uptake of Pb, as the removal efficiency of Pb showed no obvious difference when the pH changed from 5 to 6.8.

Effect of Co-existence Ions

Competitive biosorption is a common phenomenon examined with various biosorbents for metal uptake [25]. The distinct characteristics of binding sites and certain functional groups on biosorbent surfaces result in high selectivity towards metal biosorption [25]. Figure 2 showed the results of competitive biosorption for the multi-metals solution using watermelon rind as a novel biosorbent. It was found that watermelon rind selectively absorbed Pb during the entire biosorption process with limited amount of Cu adsorbed. However, the uptake of Zn became neglected and the maximal removal efficiency was found to be less than 10%. The maximum capacity of Pb adsorbed was about ten times higher than that of Zn adsorbed (Table 1), indicating that watermelon rind was in favor of Pb biosorption. These results showed that watermelon rind might be considered as a novel candidate for the separation of Pb from wastewater as it favored to absorb Pb. Besides, from Table 1, it was also found that the co-existence of these metals reduced the maximum biosorptive capacities of watermelon rind for all three metals, with the uptake of Zn being inhibited to the greatest extent.

Adsorption Isotherms

Langmuir, Freundlich, and Redlich–Peterson adsorption isotherms were used to depict equilibrium data of metals adsorbed onto watermelon rind. Isotherm parameters and correlation coefficient values were derived from the fitting of experimental data and were given in

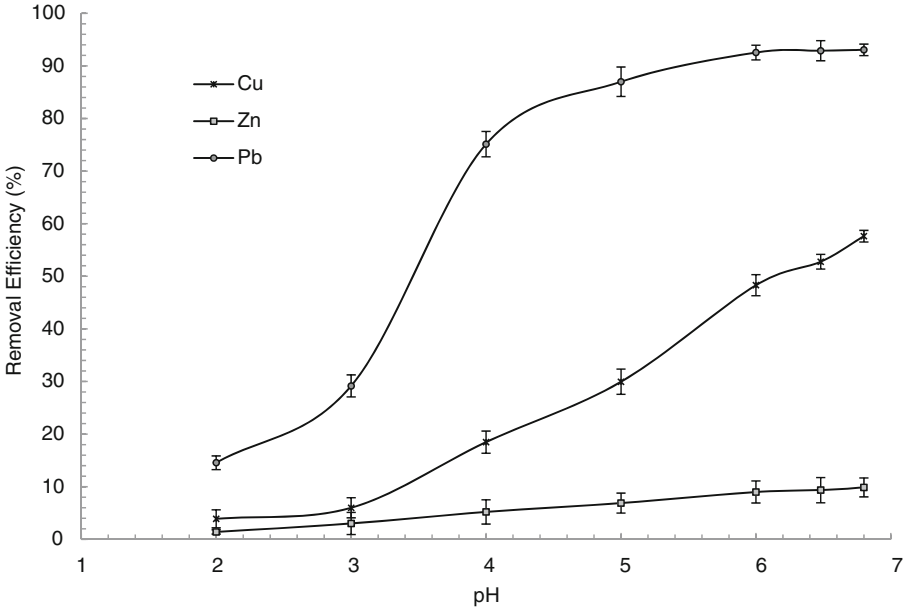

Fig. 2 Effect of solution pH on removal efficiency using watermelon rind as a novel biosorbent in multi-metals solution (dosage, 0.5 g; initial metal concentration, 10 mg/L; particle size, <150 μm; contact time, 10 h; 125 rpm; 20 °C)

Table 1 Comparison of removal efficiency of three metals in single-metal solution and multi-metals solution using watermelon rind as a novel biosorbent (pH, 6.48; initial metal concentration, 10 mg/L; particle size, <150 μm; contact time, 10 h; 125 rpm; 20 °C)

Metal type	Maximal removal efficiency (%)	Equilibrium time (h)
Cu in single-metal solution	58.4	1
Cu in multi-metals solution	55.6	1–2
Zn in single-metal solution	63.2	1
Zn in multi-metals solution	9.87	1–2
Pb in single-metal solution	99.9	1
Pb in multi-metals solution	93.1	1

Table 2. The results indicated that equilibrium had been reached within 60 min. Biosorptive capacities of Cu, Zn, and Pb were determined to be 6.281, 6.845, and 98.063 mg/g, respectively, in the present experimental conditions. The higher correlation coefficients showed that Langmuir isotherm was very suitable for describing the biosorption equilibrium of these three metals on watermelon rind. For Redlich–Peterson adsorption isotherm, since the MATLAB program was used to derive the isotherm constants by maximizing the linear correlation coefficient r^2, it was unsurprising that in all cases the Redlich–Peterson isotherms exhibited higher r^2 values, indicating that it produced a considerably better fit compared to the preceding two-constant isotherms (Langmuir and Freundlich adsorption isotherms). For instance, for Cu and Zn biosorption on watermelon rind, Redlich–Peterson isotherm was the most suitable adsorption isotherm for the data, followed by the Langmuir and then Freundlich adsorption isotherm. On the other hand, for Pb biosorption on watermelon rind, the Redlich–Peterson adsorption isotherm was still the most suitable isotherm, followed by the Freundlich and then the Langmuir adsorption isotherm.

Kinetic Models

For designing batch biosorption systems, prediction of biosorption rate plays a critical role, and information on the kinetics of metal uptake is very important for selecting optimum operating conditions for full-scale batch process and industrial-scale application [26]. Pseudo-first-order kinetic and pseudo-second-order kinetic models were used to fit the kinetic data of metals sorbed on watermelon rind. A comparison of major parameters between pseudo-first-order and pseudo-second-order kinetic models is depicted in Table 3. It was found that the higher proportion of the heavy metal ions had been adsorbed during the first 10 min of contact. The coefficient of correlation for the second-order kinetic model was

Table 2 Langmuir and Freundlich isotherm constants for the biosorption of three metals using watermelon rind as a novel biosorbent

Metal	q_m (exp)	Langmuir			Freundlich			Redlich–Peterson			
		q_m (cal)	K_a	r^2	K_F	n	r^2	g	A	B	r^2
Cu	6.252	6.281	0.636	0.999	5.735	64.10	0.990	0.999	18.92	3.05	0.9999
Zn	6.812	6.845	0.576	0.998	5.149	37.59	0.969	0.998	12.51	1.86	0.9999
Pb	92.883	98.063	0.112	0.928	39.61	4.58	0.810	0.993	55.47	0.68	0.9531

Table 3 Kinetic parameters of the pseudo-first-order and pseudo-second-order kinetic models for biosorption of three metals using watermelon rind as a novel biosorbent

Metal type	q_{eq} (exp)	Pseudo-first-order kinetics			Pseudo-second-order kinetics		
		K_1	q_{eq} (cal)	r^2	K_2	q_{eq} (cal)	r^2
Cu	5.671	0.0132	1.366	0.968	0.161	5.447	0.998
Zn	6.111	0.0118	1.096	0.960	0.202	5.889	0.999
Pb	6.492	0.0025	0.665	0.886	1.181	6.002	0.999

approximately equal to 1 and the estimated values of q_e also agreed with the experimental ones. Both facts suggested that the biosorption of these three metals followed the second-order kinetic model. Based on the results, watermelon rind was found to have a great potential to become a useful biosorbent for the removal of heavy metals from aqueous solutions.

Non-linear Regression

The chi-square statistic correlation coefficient χ^2 was obtained and the comparison between χ^2 and correlation coefficient of linear models r^2 is shown in Table 4. Among adsorption isotherms, in the non-linear analysis, Redlich–Peterson and Freundlich isotherms exhibited lower χ^2 values and were considered to be a better fit compared with Langmuir adsorption isotherm. Figure 3 showed the detailed results. Isotherm plots and the experimental data, Langmuir isotherms, the Freundlich isotherm, and the Redlich–Peterson isotherm were exhibited, respectively. Therefore, drawing conclusions from the non-linear chi-square analysis, for Cu and Zn biosorption, Langmuir adsorption isotherm was determined to be the most suitable one, followed by Redlich–Peterson adsorption isotherm for this sorption

Table 4 Comparison of linear regression correlation coefficients r^2 and non-linear regression coefficients χ^2

Model	Metal type	Isotherm	r^2	χ^2
Equilibrium	Cu	Langmuir	0.999	0.913
		Freundlich	0.972	7.735
		Redlich–Peterson	0.9999	1.668
	Zn	Langmuir	0.999	1.277
		Freundlich	0.886	7.679
		Redlich–Peterson	0.9999	1.577
	Pb	Langmuir	0.428	1221
		Freundlich	0.810	57.22
		Redlich–Peterson	0.9531	27.79
Kinetic	Cu	Pseudo-first-order	0.968	325.1
		Pseudo-second-order	0.998	0.037
	Zn	Pseudo-first-order	0.960	409.3
		Pseudo-second-order	0.999	0.315
	Pb	Pseudo-first-order	0.886	491.6
		Pseudo-second-order	0.999	1.065

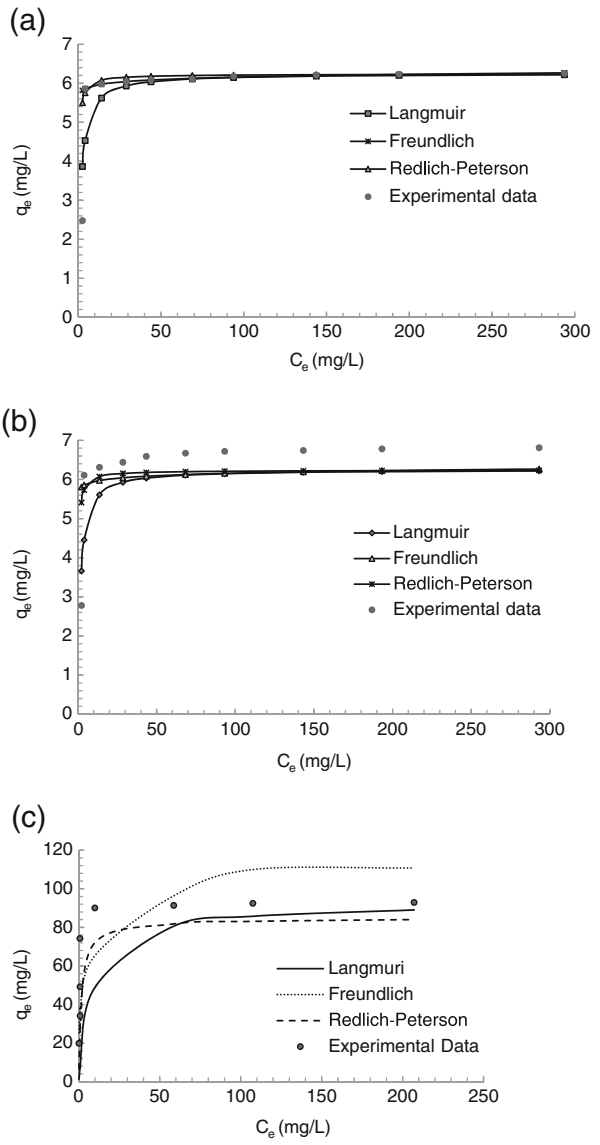

Fig. 3 Comparison of different adsorption isotherms for biosorption on watermelon rind: **a** Cu, **b** Zn, **c** Pb (pH, 6.48; dosage, 0.5 g; particle size, <150 μm; contact time, 10 h; 125 rpm; 20 °C)

system. However, for Pb biosorption on watermelon rind, Redlich–Peterson adsorption isotherm showed significant advantage. For kinetic study, extremely low χ^2 values were obtained when fitting the experimental data into pseudo-second-order kinetic model, implying that pseudo-second-order kinetic model was suitable to describe the obtained data. Detailed results were introduced in Fig. 4. Based on previous studies, unlike the linear analysis, different forms of the equation affected χ^2 values less significantly [18]. Therefore, the non-linear chi-square analysis should be considered as a method to avoid such errors.

Based on the above results, it could be found that linear regression and the non-linear chi-square analysis gave different best-fitting isotherm for the given data set, implying that a

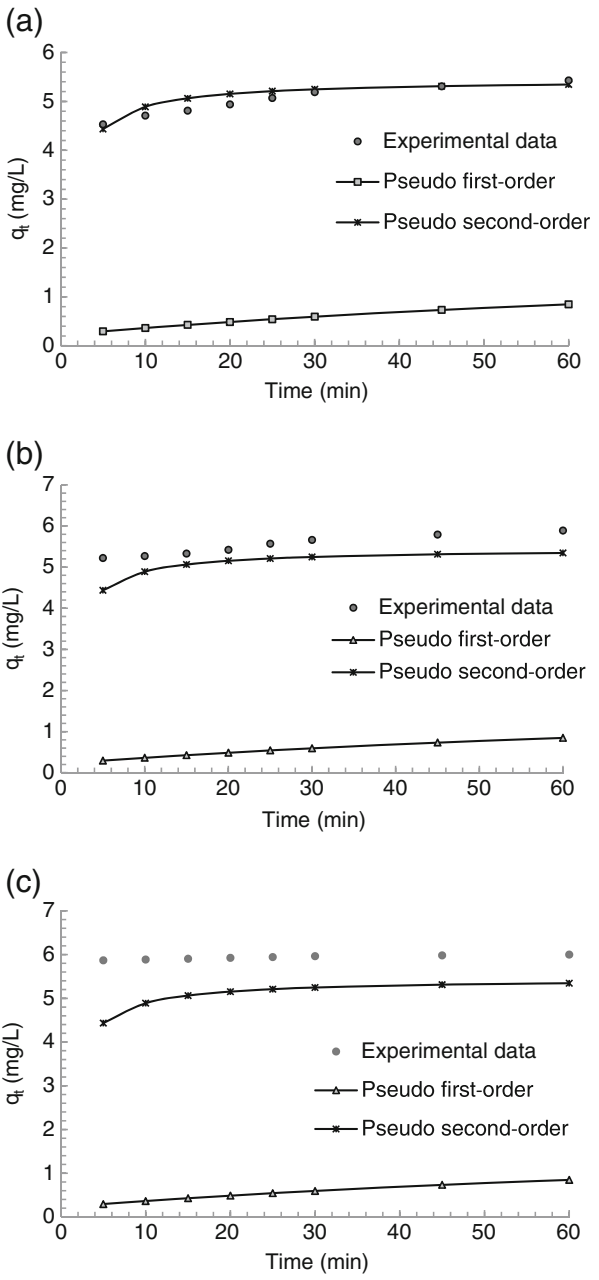

Fig. 4 Comparison of different kinetic models for biosorption on watermelon rind: **a** Cu, **b** Zn, **c** Pb (pH, 6.48; dosage, 0.1 g; initial metal concentration, 10 mg/L; particle size, <150 μm; 125 rpm; 20 °C)

significant difference existed between linear and non-linear isotherms [18]. Compared to the non-linear chi-square analysis, due to its simplicity, most of the biosorption equilibrium analysis still mostly relied on linear regression, which might have led to an inaccurate conclusion. Therefore, to ensure better results, it should be suggested that both linear and non-linear regression analyses be evaluated so as to describe the obtained data in a more comprehensive way.

Desorption Study

Desorption, i.e., to concentrate the solute, is an important part in the entire biosorption process for metal removal [10]. The efficiency of the regeneration of biosorbent after metal desorption also plays a vital role in the application of biosorption technology [27]. Therefore, regeneration of biosorbents becomes significantly necessary. In large-scale applications, regeneration of the biosorbent brings out various benefits, such as keeping the process costs down and recovering the metals extracted from the liquid phases [6, 7]. For this reason, mild and cheap eluants become desirable to achieve non-destructive recovery so as to regenerate biosorbents for further reuse in multiple cycles.

To attain the above-mentioned objective, appropriate eluants are necessary, which are closely related with the type of biosorbent and the mechanism of biosorption. At the same time, an appropriate eluant should met several requirements, such as yielding the metals in a concentrated form, no physical changes or damage to the biosorbent, and restoring the biosorbent close to the original condition for effective reuse with undiminished metal uptake [5]. Besides, being less costly, environmentally friendly, and effective are also important criteria for choosing suitable eluants [27].

In this study, four ordinary eluants were used for desorption of heavy metal ions (e.g., distilled water, 0.1 mol/L NaOH, 0.5 mol/L HON_3, and 0.5 mol/L HCl). In order to examine the reusability of this novel biosorbent, three rounds of biosorption–desorption cycle of Cu, Zn, and Pb in single-metal solution were conducted. Based on the results (Table 5), distilled water was found to be non-effective while acid eluants (e.g., HNO_3, HCl) showed significant advantages in metal recovery. Almost 100% of metals ions were recovered. However, after acid desorption, the biosorptive capacity reduced significantly in the following biosorption processes. For alkaline eluant (NaOH), it not only recovered most of the adsorbed ions but also increased the biosorptive capacity. After desorption process in NaOH solution, the removal efficiency of three metals reached as high as 99% and remained constant for all

Table 5 Desorption and resorption studies of Cu, Zn, and Pb from watermelon rind in single-metal solutions using various eluants: distilled water, 0.1 mol/L NaOH, 0.5 mol/L HNO_3, and 0.5 mol/L HCl (pH, 6.48; initial metal concentration, 10 mg/L; particle size <150 μm; contact time 10 h; 125 rpm; 20 °C)

Eluant	Metal type	First cycle		Second cycle		Third cycle	
		Metal sorbed (mg)	Metal Desorbed (mg)	Metal Resorbed (mg)	Metal Desorbed (mg)	Metal Resorbed (mg)	Metal Desorbed (mg)
Distilled water	Cu	5.862	0.158	2.859	0.148	1.801	0.158
	Zn	6.111	0.165	4.892	0.168	3.481	0.169
	Pb	9.956	0.235	9.289	0.227	9.188	0.222
NaOH	Cu	5.862	2.319	9.935	5.827	9.965	5.837
	Zn	6.111	2.581	9.942	6.847	9.957	6.792
	Pb	9.956	7.148	9.958	7.211	9.999	7.182
HNO_3	Cu	5.862	5.293	0.482	0.321	0.248	0.137
	Zn	6.111	5.892	0.473	0.304	0.222	0.108
	Pb	9.956	9.789	0.945	0.742	0.666	0.518
HCl	Cu	5.862	4.525	2.524	1.898	1.278	0.998
	Zn	6.111	5.292	3.072	2.563	0.892	0.563
	Pb	9.956	9.128	2.487	1.952	1.689	1.210

Table 6 Desorption and resorption studies of Cu, Zn, and Pb from watermelon rind in multi-metals solutions using various eluants: distilled water, 0.1 mol/L NaOH, 0.5 mol/L HNO_3, and 0.5 mol/L HCl (pH, 6.48; initial metal concentration, 10 mg/L; particle size <150 μm; contact time 10 h; 125 rpm; 20 °C)

Eluant	Metal type	First cycle		Second cycle		Third cycle	
		Metal sorbed (mg)	Metal Desorbed (mg)	Metal Resorbed (mg)	Metal Desorbed (mg)	Metal Resorbed (mg)	Metal Desorbed (mg)
Distilled water	Cu	5.277	0.111	4.114	0.116	3.187	0.115
	Zn	0.987	0.541	0.618	0.329	0.428	0.239
	Pb	9.305	0.187	9.208	0.186	9.158	0.185
NaOH	Cu	5.277	0.411	9.944	6.608	9.743	6.548
	Zn	0.987	0.884	9.752	6.508	9.684	6.444
	Pb	9.305	7.064	9.921	7.492	9.948	7.462
HNO_3	Cu	5.277	4.984	0.489	0.286	0.289	0.111
	Zn	0.987	0.956	0.217	0.111	0.117	0.052
	Pb	9.305	9.108	0.849	0.697	0.542	0.428
HCl	Cu	5.277	4.421	0.589	0.279	0.388	0.154
	Zn	0.987	0.649	0.456	0.234	0.218	0.145
	Pb	9.305	8.905	2.041	1.723	1.542	1.008

consecutive cycles. These results showed that watermelon rind could be repeatedly used in biosorption process when alkaline eluants were used.

For comparison and better understanding of desorption characteristics, desorption and re-biosorption studies of Cu, Zn, and Pb in multi-metals solution were also carried out. As can be seen from Table 6, the results showed very similar trends as the results obtained in single-metal solution. Differently from the biosorption process, there was no significant competition between these three metals during the desorption process. Besides, there was one more thing to point out. After desorption of NaOH, the removal of heavy metals became complete for all the three metals in the multi-metals solution even in the third biosorption–desorption

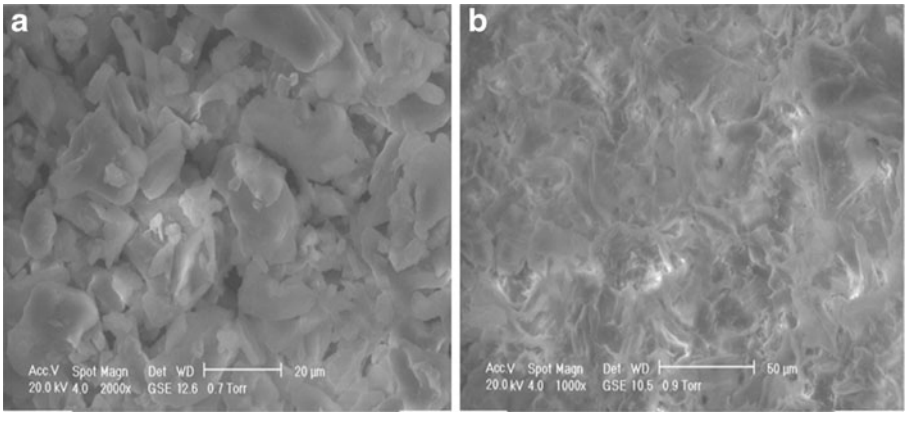

Fig. 5 Scanning electron micrographs of watermelon rind before and after biosorption process: **a** before biosorption, **b** after biosorption

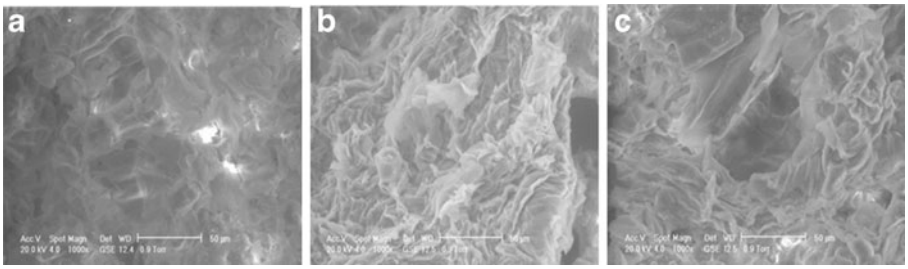

Fig. 6 Scanning electron micrograph of watermelon rind after desorption process using various eluants: **a** distilled water, **b** alkali solution, **c** acid solution

cycle. Therefore, compared to other eluants, NaOH was considered as the most suitable eluant in either single-component or multi-component solutions.

Characterization of Biosorbent

Scanning electron microscopy was used for characterizing the morphology and structure of the biosorbent. SEM micrographs of unloaded and loaded biosorbent are shown in Fig. 5. Three SEM micrographs of watermelon rind after desorption process are shown in Fig. 6. Over the biosorption period, the morphology of the biosorbent had undergone a remarkable physical change. Figure 5 represented the integrated and cluster arrangement that occurred before and after biosorption which clearly showed that metal particles adhere on the surface of the biosorbent as the pores on the surface area became much less and smaller. Besides, it was found that after contacting with metal ions, the active surface area increased, which had been covered by precipitated metal ions. After desorption of distilled water, it was found that some pores re-occurred on the surface, explaining the phenomenon that the powder can still absorb some metal ions after desorption process in distilled water. After desorption process of NaOH solution, more hydroxyl ligands were believed to attach to the surface area, whing means that more micro-precipitation occurred on the biosorbent surface, and therefore the removal efficiency had been increased significantly. On the contrary, after desorption process of acid solution, the biosorptive capacity of watermelon rind became neglected due to the fact that there was no functional group on the surface area that could exchange with metal ions in the solution. Based on the above analysis, ion exchange and micro-precipitation which occurred on the surface area were believed to be the main biosorption mechanism.

The textural parameters of various biosorbents (raw biosorbent, biosorbent after biosorption process, and biosorbent after NaOH desorption process) were summarized in Table 7. The BET

Table 7 Pore properties of various biosorbents (e.g., raw biosorbent, biosorbent after sorption process, and biosorbent after NaOH desorption process)

Property	Raw biosorbent	Biosorbent after sorption process	Biosorbent after NaOH desorption process
BET surface area (m^2/g)	5.97	15.55	82.87
Micro-pore area (m^2/g)	14.15	3.87	3.96
Micro-pore volume (cm^3/g)	0.01	0.01	0.01
Mean micro-pore diameter (nm)	87.1	87.2	87.0

surface area of biosorbents after biosorption process (15.55 m^2/g) was larger than that of raw biosorbent (5.97 m^2/g). Similar results were found in the biosorbent after desorption process (82.87 m^2/g), the area of which was even larger than the biosorbent after biosorption process. This result explained well the phenomenon that after NaOH desorption process the biosorptive capacity of watermelon rind increased significantly. The percentage of micro-pore area for the biosorbent after biosorption and desorption process was 27.35% and 27.96% of the raw biosorbent, respectively. From this result, the biosorbent after biosorption process was more homogenized than that of raw biosorbent, which confirmed the monolayer biosorption formed for heavy metals onto the surface of watermelon rind.

Conclusions

- Powdered watermelon rind was demonstrated to be an effective biosorbent in removing Cu, Zn, and Pb, especially for Pb removal, and had high desorption capacity with NaOH as eluant.
- After desorption of NaOH, dried watermelon rind remained to demonstrate excellent biosorptive capacity either in single-metal or multi-metals solution.
- Metal uptake performance of watermelon rind was strongly affected by pH.
- Langmuir isotherm model was suitable to describe the biosorption process, and biosorption kinetic was found to be the best-fit pseudo-second-order equation.
- Ion exchange and micro-precipitation which occurred on the surface area were estimated to be the main biosorption mechanisms.

Acknowledgement This research was partially funded by the UTS Early Career Research Grant.

References

1. Uauy, R., Olivares, M., & Gonzalez, M. (1998). *Clinical Nutrition, 67*, 952–959.
2. Wang, B., Feng, W.-Y., Wang, T.-C., Jia, G., Wang, M., Shi, J.-W., Zhang, F., Zhao, Y.-L., & Chai, Z.-F. (2006). *Toxicology Letters, 161*, 115–123.
3. Wang, Q., Zhao, H. H., Chen, J. W., Gu, K. D., Zhang, Y. Z., Zhu, Y. X., Zhou, Y. K., & Ye, L. X. (2009). *Science of the Total Environment, 407*, 5986–5992.
4. Park, D., Yun, Y.-S., & Park, M. J. (2010). *Biotechnology and Bioprocess Engineering, 15*, 86–102.
5. Ahalya, N., Ramachandra, T. V., & Kanamadi, R. D. (2003). *Chemical Engineering Science, 7*, 71–79.
6. Volesky, B. (1987). *Trends in Biotechnology, 5*, 96–101.
7. Jang, L. K., Nguyen, D., & Geesey, G. G. (1998). *Water Research, 29*(1), 315–321.
8. Benjamin, M. M., Sletten, R. S., Bailey, R. P., & Bennet, T. (1996). *Water Research, 30*, 2609–2620.
9. Dean, J. G., & Bosqui, F. L. (1972). *Environmental Science and Technology, 6*, 518–521.
10. Wang, J. L., & Chen, C. (2009). *Biotechnology Advances, 27*, 195–226.
11. Ferraz, A. I., & Teixeira, I. A. (1999). *Bioprocess Engineering, 21*, 431–437.
12. Rimando, A. M., & Perkins-Veazie, P. (2005). *Chromatogr A, 1078*, 196–200.
13. USDA National Nutrient Database for Standard Reference 2004. Available from http://www.usda.gov/wps/portal/usda/usdahome
14. Langmuir, I. (1918). *American Chemical Society, 40*(9), 1361–1403.
15. Freundlich, H. (1906). *Physical Chemistry, 57*, 385–470.
16. Redlich, O., & Peterson, D. L. (1959). *Physical Chemistry, 63*, 1024.
17. Lagergren, S. (1898). *Handlingar, 24*(4), 1–39.
18. Ho, Y. S. (2004). *Scientometrics, 59*(1), 171–177.

19. Ho, Y. S., & McKay, G. (1998). *Chemical Engineer, 70*(2), 115–124.
20. Ho, Y. S. (2006). *Hazard Mater, 136*(3), 681–689.
21. Sankaran, M. (1959). *Biometrika, 46*, 235–237.
22. Esposito, A., Pagnanelli, F., & Veglio, F. (2002). *Chemical Engineering Science, 57*, 307–313.
23. Volesky, B., & Holan, R. Z. (1995). *Biotechnology Progress, 11*, 235–250.
24. Al-Qodah, Z. (2006). *Desalination, 196*, 164–176.
25. Kadirvelu, K., Goel, J., & Rajagopal, C. (2008). *Hazard Mater, 153*, 502–507.
26. Pandey, P. K., Sharma, S. K., & Sambi, S. S. (2010). *Environmental Science and Technology, 7*, 395–404.
27. Vijayaraghavan, K., & Yun, Y.-S. (2008). *Biotechnology Advances, 26*, 266–291.